

Grain-boundary-controlled transport in GaN layers

I. Shalish, L. Kronik, G. Segal, and Yoram Shapira

Department of Physical Electronics, Tel-Aviv University, Ramat-Aviv 69978, Israel

S. Zamir, B. Meyler, and J. Salzman

Department of Electrical Engineering, Solid State Institute and Microelectronics Research Center,

Technion—Israel Institute of Technology, Haifa 32000, Israel

(Received 23 April 1999)

An exponential dependence of the photoconductivity on the surface photovoltage at GaN layers is predicted theoretically and confirmed experimentally. The prediction is based on the assumption that the material is mainly an ordered polycrystal, consisting of columnar grains. Accordingly, transport is expected to be limited by potential barriers at the grain boundaries, arising from the charge trapped at grain-boundary defects. The observed exponential dependence provides evidence that strongly supports the model by establishing a direct link between the *bulk* conductivity and the *surface* potential barrier. The same model is shown to successfully explain several other defect-related findings as well.

In recent years, technological breakthroughs in GaN growth, doping, and contacting technologies have resulted in numerous devices, notably the blue GaN-based laser.¹ Progress, however, is still challenged by a high density of defects.² A typical finding is a columnar grain structure often observed in cross-sectional micrographs.² The effect of grain boundaries on transport in other semiconductors, especially polycrystalline Si, has been extensively studied.³ It is widely accepted that trapped charge at grain-boundary interface states leads to the formation of potential barriers and depletion regions, as shown schematically in Fig. 1. These potential barriers resist intergrain transport, a hypothesis successfully used for explaining Hall⁴ and ion-implantation⁵ experiments in GaN films. If this mechanism is in effect, it can inclusively explain several intriguing transport-related phenomena observed at GaN layers, such as: (i) a persistent and nonexponentially decaying photoconductivity (PC),^{6,7} (ii) a huge ultraviolet gain of GaN-based photodetectors,^{8,9} (iii) in ion-implanted films, a highly superlinear decrease of film conductivity with increasing implanted ion dose,⁵ and (iv) an increasing mobility with increasing carrier concentration, rather than the usual decrease.⁴ In this paper, we present more direct evidence for grain-boundary limited transport in GaN, using surface photovoltage and photoconductivity measurements. We then rationalize the above-mentioned transport phenomena.

Assuming a thermionic emission over a barrier and a small applied bias (i.e., an effective bias much smaller than the thermal voltage across each grain), barrier-limited transport is characterized by an exponential dependence of the conductivity, σ , on the average grain-boundary barrier height ϕ_{gb} .^{3,10}

$$\sigma = \sigma_0 \exp(-q\phi_{gb}/kT), \quad (1)$$

where σ_0 is a proportionality coefficient, q is the (absolute value of the) electron charge, k is the Boltzmann constant, and T is the temperature.

To directly establish the applicability of Eq. (1) to our case, one needs to modify and measure the potential barriers at the grain boundaries. The latter can be conveniently modified by the photovoltaic effect, i.e., $\phi_{gb} \equiv \phi_{gb}^0 - \Delta\phi_{gb}$, where ϕ_{gb}^0 is the potential barrier in the dark, and $\Delta\phi_{gb}$ is the photoinduced lowering of this potential barrier. Equation (1) can therefore be expressed as

$$\sigma = \sigma_0 \exp(-q\phi_{gb}^0/kT) \exp(q\Delta\phi_{gb}/kT). \quad (2)$$

Practically, an illumination-insensitive shunt component σ_{sh} may be observed, especially because light chopping was avoided in the experiment given below.¹¹ In addition, transport across potential barriers is not always strictly thermal, and transport measurements involve averaging over potential barrier inhomogeneities. Therefore, it is common practice to introduce a transport-related ideality factor¹² η_t so that Eq. (2) is modified to the form

$$\sigma = \sigma_{sh} + \sigma_0 \exp(-q\phi_{gb}^0/kT) \exp(q\Delta\phi_{gb}/\eta_t kT). \quad (3)$$

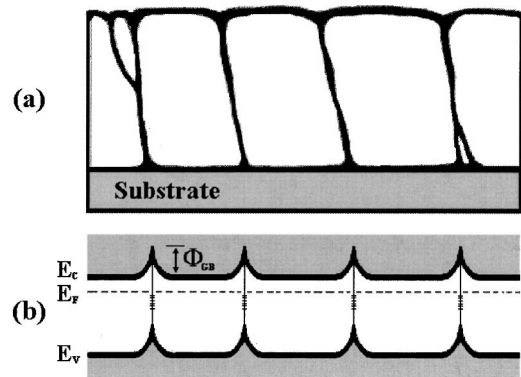


FIG. 1. (a) A schematic diagram of a film possessing a columnar grain structure. (b) A schematic view of the corresponding equilibrium band diagram (ϕ_{gb} —the average grain-boundary potential barrier).

Unfortunately, while ϕ_{gb} is easily *modified*, a direct *measurement* of $\Delta\phi_{gb}$ is a nontrivial task.¹³ If, on the other hand, ϕ_{gb} can be related to the *surface* potential barrier ϕ_s , this problem can be circumvented, because the surface potential can be both controlled *and* monitored by the surface photovoltage (SPV) technique.^{14,15} To obtain such a relation, we now solve the Poisson equation under the depletion approximation.^{3,16} From charge conservation considerations, we obtain

$$Q_s = qN_d w_s, \quad (4a)$$

$$Q_{gb} = 2qN_d w_{gb}, \quad (4b)$$

where Q_s (Q_{gb}) and w_s (w_{gb}) are the surface (grain boundary) trapped charge density and space-charge region width, respectively, and N_d is the doping level of the layer. The factor of 2 difference between the right-hand sides of Eqs. (4a) and (4b) arises because the surface-trapped charge supports *one* space-charge region (SCR), whereas the grain-boundary trapped charge supports *two* SCR's (one on each side of the boundary). Solving the Poisson equation to relate the potential barriers to the grain-boundary heights, we obtain

$$\phi_s = qw_s^2/2\epsilon; \quad \phi_{gb} = qw_{gb}^2/2\epsilon, \quad (5)$$

where ϵ is the permittivity of the film. Finally, inserting Eq. (4) in Eq. (5) we obtain

$$\phi_s = Q_s^2/2\epsilon qN_d; \quad \phi_{gb} = Q_{gb}^2/8\epsilon qN_d. \quad (6)$$

If the defect state density and energy distribution at the free surface are the same as those of the grain boundary (an assumption which is corroborated below), then $Q_s \cong Q_{gb}$, and Eq. (3) yields

$$\phi_s = 4\phi_{gb}, \quad (7)$$

which leads to:

$$\Delta\phi_{gb} = \Delta\phi_s/4\eta_I, \quad (8)$$

where η_I is an illumination-related ideality factor.¹⁷ $\Delta\phi_s$ is, by definition, equal to the SPV.¹⁴ Combining Eqs. (3) and (8), we obtain an explicit relation between the conductivity and the SPV ($\equiv \Delta\phi_s$) measured under identical conditions:

$$\sigma = \sigma_{sh} + \sigma_0 \exp(-q\phi_{gb}^0/kT) \exp(q\Delta\phi_s/4\eta_I kT), \quad (9)$$

where $\eta \equiv \eta_I \eta_I$ is the overall ideality factor. Equation (9) provides for our main prediction: if the surface and grain-boundary defect structures are similar, grain-boundary limited transport implies an *exponential* relation between the conductivity and the *surface* potential barrier.¹⁸

To test this prediction, PC and SPV measurements were performed on various GaN layers, under identical illumination conditions, as well as photoluminescence (PL) measurements. All samples studied in this work were grown using metal-organic vapor-phase epitaxy on (0001)-oriented sapphire substrates.¹⁹ Soldered In contacts, used as Ohmic contacts, were verified to be Ohmic using current-voltage measurements. For eliminating any residual contact resistance effects, a four-contact arrangement was used.⁶ Here we present results obtained from three representative samples,

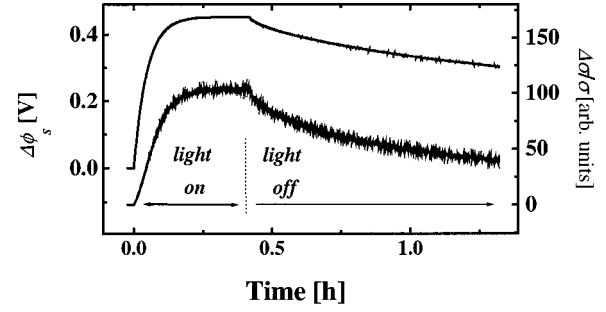


FIG. 2. Time-resolved photoconductivity (bottom) and surface photovoltage (top) curves, obtained from sample 1 upon switch-on and switch-off of illumination by 2.5 eV photons.

denoted 1–3 below. The sample thicknesses were $\sim 0.2 \mu\text{m}$ (1) and $\sim 3 \mu\text{m}$ (2 and 3). The samples exhibited an *n*-type conductivity corresponding to an unintentional doping level of $n \sim 5 \times 10^{17} \text{cm}^{-3}$.

Persistent PC *and* SPV behavior were observed in all samples studied. A typical example is given in Fig. 2, which features the illumination switch-on and switch-off PC and SPV responses to illumination by 2.5 eV photons. PC $= f(\text{SPV})$ curves were constructed using pairs of PC and SPV values, corresponding to the same time after illumination switch-off. The resulting curves are shown in Fig. 3. All three samples indeed feature the exponential dependence predicted in Eq. (9), with overall ideality factors ranging from 1.17 to 1.78.

Prima facie, Fig. 3 provides a quantitative confirmation of the prediction made in Eq. (9), and therefore strongly corroborates the model given. For obtaining additional insight into the model, we now turn to discussing the *nature* of the similarity between surface and grain-boundary states. We then discuss *how* these states are related to the persistence of the SPV and PC, respectively.

Independent measurements using PL, PC, and SPV spectroscopies are shown in Fig. 4. The PL spectra [Fig. 4(a)] feature a band-gap-related peak at $\sim 3.4 \text{ eV}$ (to which these spectra have been normalized). In addition, they feature a broad sub-band-gap peak, centered at $\sim 2.2 \text{ eV}$. This is the

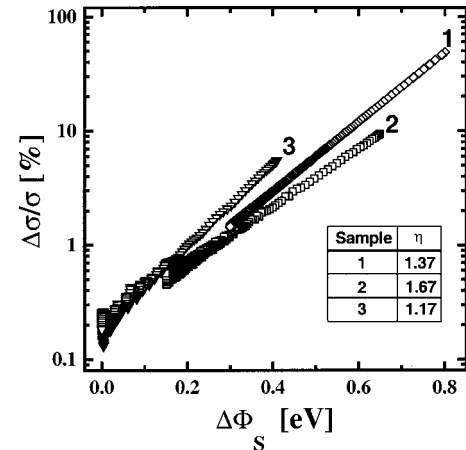


FIG. 3. Photoconductivity vs surface photovoltage curves of the three representative samples. A constant term was subtracted from the photoconductivity values for elucidating the exponential nature of the dependence.

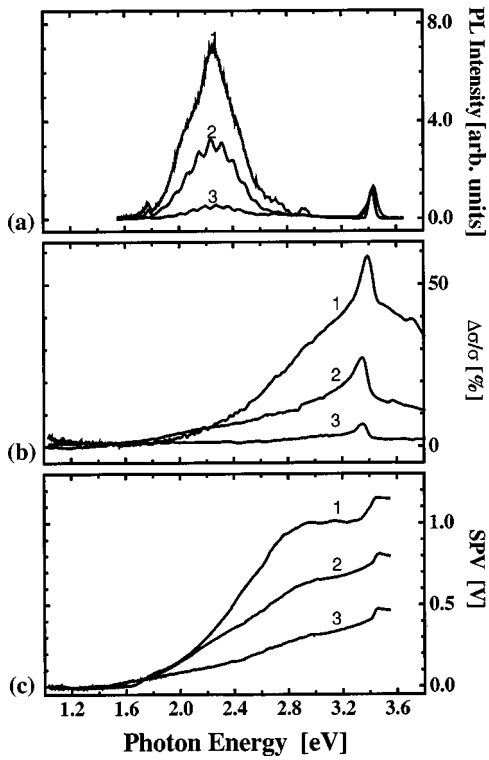


FIG. 4. (a) Photoluminescence, (b) photoconductivity, and (c) surface photovoltage spectra of the three representative samples.

well-known “yellow luminescence” (YL) peak, resulting from defect states, shown to be distributed ~ 2.2 eV below the conduction-band edge.^{19–21} As shown in Fig. 4a, the samples chosen for this study exhibited *varying* ratios of YL to band-edge emission, so as to ascertain the general nature of our conclusions.

A band-gap-related peak at ~ 3.4 eV is also observed at the PC spectra (Fig. 4b). Here, a *peak* (rather than a “knee”) is observed because at photon energies exceeding the band gap, the absorption coefficient increases considerably, and most photons are absorbed in a thin near-surface layer. Thus, many generated electron-hole pairs are lost to surface recombination, and the net excess carrier is *decreased* rather than *increased*.²² This confirms that we have indeed probed the *bulk* photoconductivity rather than the *surface* one. In the sub-band-gap energy range, the PC data feature a significant signal starting at ~ 1.6 eV, i.e., at the onset of the YL. Moreover, the magnitude of the yellow response in the PC spectra increases with increasing yellow response in the PL data. Indeed, it was previously established that PC probes the yellow absorption.⁶ This absorption involves the transition inverse to that of the YL, i.e., the excitation of electrons from the deep state into the conduction band.

A band-gap-related feature at ~ 3.4 eV is also observed in the SPV spectra [Fig. 4(c)]. However, because SPV probes a surface quantity, this band-gap-related feature is typically observed as a knee rather than a peak.¹⁴ Just like the PC data, the SPV data also feature a significant signal starting at ~ 1.6 eV, which correlates with the PL data. Therefore, SPV also probes the yellow absorption. However, whereas PC is by nature a *bulk*-sensitive tool, SPV measurements of such GaN layers are sensitive to states situated at the free GaN *surface*.¹⁹

The SPV and PC data are easily reconciled if one assumes that the YL-related states are not homogeneously distributed in the bulk but rather are situated primarily at grain boundaries, as well as in other extended defects. Indeed, YL-related states have been assigned to extended defects and grain boundaries.^{2,23,24} The similarity of the SPV and PC results therefore suggests that, in this case, the free surface may be considered a special case of a grain boundary. From this point of view, the defect energy distributions at the grain boundaries and at the free surface should be comparable. Thus, the assumption $Q_s \cong Q_{gb}$ leading to Eq. (9), is plausible *a priori* and not only justified *a posteriori* by the results of Fig. 3. Moreover, we can use the SPV magnitude as a lower limit for the surface potential¹⁷ and divide the result by 4 to obtain an estimate for the grain-boundary barrier height. This yields a highly reasonable value that is of the order of 150 meV to 250 meV, depending on the sample.

Recent studies have shown conclusively that the persistent PC is associated with the YL-related states.^{6,7} For this reason, yellow, 2.5 eV photons were used as the illumination source in this study. The relation between the YL and the persistent PC is easily interpreted within the framework of the grain-boundary limited transport model. First, we have previously shown that the YL-related defects are of an *acceptor* nature and are negatively charged in equilibrium.¹⁹ If these states are present at the grain boundaries of an *n*-type material, their negative charge will induce grain-boundary potential barriers that resist lateral conductivity. Discharging these states induces a conductivity increase, brought about by lowering the barriers. Such a discharge may take place when the film is illuminated at a photon energy sufficient to excite electrons from these states into the conduction band (i.e., yellow illumination). This is because the excited electrons are swept into the grain by the electric field of the SCR. When the illumination is switched off, electrons from the bulk can only use the thermal energy in order to surmount the remaining potential barrier, refill the grain-boundary states, and resume their equilibrium distribution. Furthermore, during this process the barrier height, and consequently the trapping process lifetime, progressively increase, resulting in a *persistent* PC.

The same model predicts that persistent PC behavior *must* be accompanied by persistent SPV behavior, as indeed observed in all samples, due to a similar excitation of YL-related states situated at the *free surface*. Moreover, the SPV decay is expected to be slower than that of the PC, because the surface potential barrier that electrons must surmount is higher than that at the grain boundary [Eq. (7)]. Indeed, a slower decay of the SPV, with respect to that of the PC, is apparent in Fig. 2.

We note that in a different model persistent PC in GaN films has been related to metastable states induced by large lattice relaxations.²⁵ Interestingly, while this mechanism is highly plausible, in light of what is known for other III–V compounds,²⁶ Fig. 2 rules out its dominance for the films studied here. The surface potential and the bulk doping are inversely related [Eq. (6)]. Therefore, had the persistence of the SPV been associated with a persistent increase in bulk doping, the time constant associated with the PC and SPV decays would have been *the same*. This is clearly not the case here. Indeed, Lang noted that even in III–V alloys,

where persistent PC due to metastable states is well known, persistent PC due to macroscopic potential barriers, if present, “cannot be dismissed lightly.”²⁶

The model we have corroborated can also account for the other transport phenomena listed above. The huge ultraviolet gain can be related to a sharp increase in the effective carrier mobility, brought about by the photoinduced reduction of ϕ_{gb} [Eq. (1)].²⁷ The highly nonlinear dependence of the conductivity on implantation dose can be brought about because the implantation causes a decrease in the effective bulk doping due to a controlled introduction of defects.⁵ This increases ϕ_{gb} [Eq. (6)] and therefore reduces σ exponentially [Eq. (1)]. Finally, the same increase of ϕ_{gb} with decreasing effective doping can explain the decrease in effective mobility with decreasing doping level.⁴

In conclusion, we have presented a model for grain-boundary controlled transport, according to which transport is limited by potential barriers associated with grain boundaries. The similarity of the defect energy structure at the free surface and at the grain boundary of GaN layers allowed us to use the free surface potential as an indicator of the grain-boundary potential. This allowed for significant experimental support of the model, obtained by observing a persistent surface photovoltage behavior and an exponential dependence of the photoconductivity on the surface photovoltage. These findings provide significant qualitative and quantitative evidence, respectively, in support of the model.

We thank Professor K. Weiser and Professor R. Kalish for their illuminating remarks. This research was supported in part by the Israel Ministry of Science and by the Kidron Fund for Research in Microelectronics. Y. S. is grateful to Henry and Dinah Krongold for their generous support.

-
- ¹S. Nakamura and G. Fasol, *The Blue Laser Diode—GaN Based Light Emitters and Lasers* (Springer-Verlag, Berlin, 1997).
- ²F. A. Ponce and D. P. Bour, *Nature (London)* **386**, 351 (1997).
- ³J. Y. W. Seto, *J. Appl. Phys.* **46**, 5247 (1975).
- ⁴M. Fehrer, S. Einfeldt, U. Birkle, T. Gollnik, and D. Hommel, *J. Cryst. Growth* **189/190**, 763 (1998).
- ⁵C. Uzan-Sagui, J. Salzman, R. Kalish, V. Richter, U. Tisch, and S. Zamir, *Appl. Phys. Lett.* **74**, 2442 (1999).
- ⁶H. M. Chen, Y. F. Chen, M. C. Lee, and M. S. Feng, *Phys. Rev. B* **56**, 6942 (1997).
- ⁷C. V. Reddy, K. Balakrishnan, H. Okumura, and S. Yoshida, *Appl. Phys. Lett.* **73**, 244 (1998).
- ⁸F. Binet, J. Y. Duboz, E. Rosencher, F. Scholz, and V. Härle, *Appl. Phys. Lett.* **69**, 1202 (1996).
- ⁹E. Muñoz, E. Monroy, J. A. Garrido, I. Izpura, F. J. Sánchez, M. A. Sánchez-García, E. Calleja, B. Beuamont, and P. Gibart, *Appl. Phys. Lett.* **69**, 1202 (1997).
- ¹⁰L. L. Kazmerski, in *Polycrystalline and Amorphous Thin Films and Devices*, edited by L. L. Kazmerski (Academic, New York, 1980), p. 98.
- ¹¹Two mechanisms may account for the shunt effect. The first is the conductivity of the nonilluminated peripheries of the sample. The second is a possible contribution of the high conductivity of the heavily defective GaN buffer layer grown on the sapphire substrate.
- ¹²S. M. Sze, *Physics of Semiconductor Devices*, 2nd ed. (Wiley, New York, 1981), p. 264.
- ¹³M. J. Cohen, J. S. Harris, and J. R. Waldrop, in *Gallium Arsenide and Related Compounds*, edited by C. Wolfe, IOP Conf. Ser. No. 45 (Institute of Physics, London, 1979), p. 263.
- ¹⁴H. C. Gatos and J. Lagowski, *J. Vac. Sci. Technol.* **10**, 130 (1973).
- ¹⁵L. Kronik and Y. Shapira, *Surf. Sci. Rep.* **37**, 1 (1999).
- ¹⁶M. Leibovitch, L. Kronik, E. Fefer, and Y. Shapira, *Phys. Rev. B* **50**, 1739 (1994).
- ¹⁷O. B. Aphek, L. Kronik, M. Leibovitch, and Y. Shapira, *Surf. Sci.* **409**, 485 (1998).
- ¹⁸It is important to note that even if the relation $Q_s \cong Q_{\text{gb}}$ is not strictly obeyed, Eq. (9) would still predict an exponential dependence, the only difference being a numerical factor different than 4 in the exponent.
- ¹⁹I. Shalish, L. Kronik, G. Segal, Y. Rosenwaks, Y. Shapira, U. Tisch, and J. Salzman, *Phys. Rev. B* **59**, 9748 (1999).
- ²⁰T. Suski, P. Perlin, H. Teisseyre, M. Leszczynski, I. Grzegory, J. Jun, M. Bockowski, S. Porowski, and T. D. Moustakas, *Appl. Phys. Lett.* **67**, 2188 (1995).
- ²¹E. Calleja, F. J. Sánchez, D. Basak, M. A. Sánchez-García, E. Muñoz, I. Izpura, F. Calle, J. M. G. Tijero, J. L. Sánchez-Rojas, B. Beaumont, P. Lorenzini, and P. Gibart, *Phys. Rev. B* **55**, 4689 (1997).
- ²²H. B. DeVore, *Phys. Rev.* **102**, 86 (1956).
- ²³P. de Mierry, O. Ambacher, H. Kratzer, and M. Stutzmann, *Phys. Status Solidi* **A158**, 597 (1996).
- ²⁴J. Kang and T. Ogawa, *J. Mater. Res.* **13**, 2100 (1998).
- ²⁵T. Mattila, A. P. Seitsonen, and R. M. Nieminen, *Phys. Rev. B* **54**, 1474 (1996); S. J. Xu, G. Li, S. J. Chua, X. C. Wang, and W. Wang, *Appl. Phys. Lett.* **72**, 2451 (1998).
- ²⁶D. Lang, in *Deep Centers in Semiconductors*, 2nd ed., edited by S. T. Pantelides (Gordon & Breach, Philadelphia, 1992), pp. 591–641.
- ²⁷J. A. Garrido, E. Monroy, I. Izpura, and E. Muñoz, *Semicond. Sci. Technol.* **13**, 563 (1998).